Supplemental Materials

Supplemental Methods

Constructs

GST-α-appendage, GST-β2-appendage, 6His-β2-appendage and GST-β2-appendage+hinge constructs were described previously (Owen et al, 2000). For ITC experiments, thrombin cleaved α and 6Hisβ2 were used after purification by affinity resins and gel filtration. Mutations were made by PCR mutagenesis and constructs were sequenced. All the key α-appendage mutants are well folded as monitored by the stoichiometry of binding in ITC experiments. All our proteins used for ITC and biochemistry were purified via affinity resins, Q-sepharose and gel filtration before concentrating and freezing in aliquots. Thus we do not have a problem with stability over time.

6xHis human eps15-MD (530-791) (STSSSE…GKRSI) was cloned into ER1/Not1 sites of pET28c and a GST version was cloned into same sites of pGex4T2. The affinity measurement for both the GST tagged and non-GST tagged version were identical showing the GST dimerisation was not significant to our experiments. We also made constructs covering the remainder of the motif-domain and found no further high affinity binding sites.

GST rat epsin1-MD (249-401) (TGGKE…DTEPD) was cloned into ER1/Not1 sites of pGex4T2 and thrombin cleaved for ITC measurements.

GST rat epsin1-MD+ (249-410) (TGGKE…FDRLR) was cloned into ER1/Not1 sites of pGex4T2 and thrombin cleaved for ITC measurements. When cleaved the protein is partially degraded but the affinity of the 1st site which we measure accurately is still 0.15μM. This construct contain an additional FxDFxxL sequence compared to epsin1-MD.

GST rat AP180-MD (516-915) (ATAPS…IKDFL) was cloned into ER1/Not1 sites of pGex4T2 and thrombin cleaved for ITC measurements. This protein is slightly degraded and the fitting of a two site model is not fully robust. The high affinity site is most reliable.

GST rat Amph1 (1-390) (start… WTTSTD) was cloned into the ER1/Not1 sites of pGex4T1. Has DNF, DPF and WxxW adaptor binding sites and the N-terminal BAR domain which will dimerise the protein.

GST mouse Syj170-MD (1303-1567) (QVKI… to end) was cloned into the ER1/Not1 sites of pGex4T3. Has DPF, 3xNPF, FxDNF, WVxF and DNF motifs. A mutant of the first DPF to DPD was made by PCR mutagenesis.

Crystallography and structure determination

Co-crystals of α-appendage and Syj-P3 were grown by hanging-drop vapour diffusion against a reservoir containing conditions centred around 1.2M Ammonium Sulphate, 3% isopropanol and 0.05M Sodium Citrate. Hanging drops were 2μl and contained 222μM α-adaptin appendage and 277.5μM Syj-P3. Crystals were obtained after approximately 1 week of incubation at 18ºC. To obtain crystals containing both Syj-P3 and Syj P1, α-appendage – Syj-P3 co-crystals were soaked in a solution of mother liquor containing Syj-P1.

Crystals were flash-frozen in liquid nitrogen using Paratone-N (Hampton Research) as a cryoprotectant and data were collected at 100K on a rotating-anode source and at ID 14.1 ($\lambda = 0.98$Å) at the European Synchrotron Radiation Facility. Crystals were monoclinic and belonged to spacegroup C2 (a = 146.6Å, b = 67.3Å, c = 39.7Å, $\beta = 94.53$º). Data tables and further information are found in Supp. Table 2. The validated coordinates and structure factors for the crystal structure containing Syj-P3 and Syj-P1 have been deposited with the protein data bank (PDB ids: 1w80 and r1w80sf).

Isothermal Titration Calorimetry (ITC)

Binding of peptides and proteins to appendage domains and was investigated by ITC (Wiseman et al, 1989) using a VP-ITC (MicroCal Inc., USA). This technique allows us to calculate *equilibrium* association or dissociation constants for interactions. These are distinct from association and dissociation *rate* constants measured by surface plasmon resonance. As we can accurately measure the concentrations of protein/peptides used we can get accurate values for the stoichiometry of interactions. Where proteins are not a single species due to degradation then the stoichiometry may be inaccurate but the affinity can still be measured if the concentration of the ligand in the syringe is accurate. All experiments were performed in 100mM HEPES, pH 7.4, 50mM NaCl, 2mM DTT at 10°C and protein concentrations were determined by absorbance at 280nm unless otherwise stated. The peptides or proteins were injected from a syringe in 40-50 steps up to a 3-5 fold molar excess over the cell concentration. The cell contained 1.36ml protein solution and typically the ligand was added in steps of 4-8μl every 3.5min. Concentrations were chosen so that the binding partners in the cell were at least 5 fold higher than the estimated dissociation constant, if possible. The ligands in the syringe were again at least 10 fold more concentrated. The heat of dilution of the ligand was subtracted from the data prior to fitting. Titration curves were fitted to the data using the ORIGIN program supplied by the manufacturer yielding the stoichiometry N, the binary equilibrium constant K_a (= K_d^{-1}) and the enthalpy of binding. The entropy of binding ΔS was calculated from the relationship $\Delta G = -RT \ln K_a$ and the Gibbs-Helmholtz equation. Peptides were purchased at > 95 % purity from the Institute of Biomolecular Sciences, University of Southampton, UK and weighed on an analytical balance and verified by measuring the OD280 or OD257. The resulting concentration errors are estimated to be < 10 %.

Unless otherwise stated the values for the stoichiometry N were within this error region around N =1.

Transferrin uptake and immunofluorescence
Cos 7 cells were transfected using GeneJuice according to manufacturers instructions, plated onto polylysine coated coverslips 24 hours post transfection and assayed for transferrin uptake 48 hours post transfection. Cell were incubated in serum free medium for 1 hour and then incubated with 25μg/ml biotinylated transferrin for 30min at the temperature indicated. Cells were then fixed using 4% paraformaldehyde, 0.03M sucrose in PBS for 30min. Fixative was preincubated at the experimental temperature.

Cells were permeabilized with 0.2% saponin, blocked with 10% goat serum, incubated in a range of primary antibodies as indicated below, and fluorochrome conjugated streptavidin followed by fluorochrome conjugated secondary antibodies, mounted and viewed using a BioRad Radiance confocal system.

AntiMyc polyclonal from Cell Signalling, AntiMyc monoclonal Sigma 9E10, AntiAP2 monoclonal from Transduction Laboratories, AntiClathrin monoclonal X22 a kind gift from Frances Brodsky, Anti eps15 polyclonal Ra15.

Owen DJ, Vallis Y, Pearse BM, McMahon HT and Evans PR (2000) The structure and function of the beta 2-adaptin appendage domain. *EMBO J* **19:** 4216-4227
Wiseman T, Williston S, Brandts JF and Lin LN (1989) Rapid measurement of binding constants and heats of binding using a new titration calorimeter. *Anal Biochem* **179:** 131-137

Supp Fig. 1
Sequence conservation and surface accessibility of α-appendages
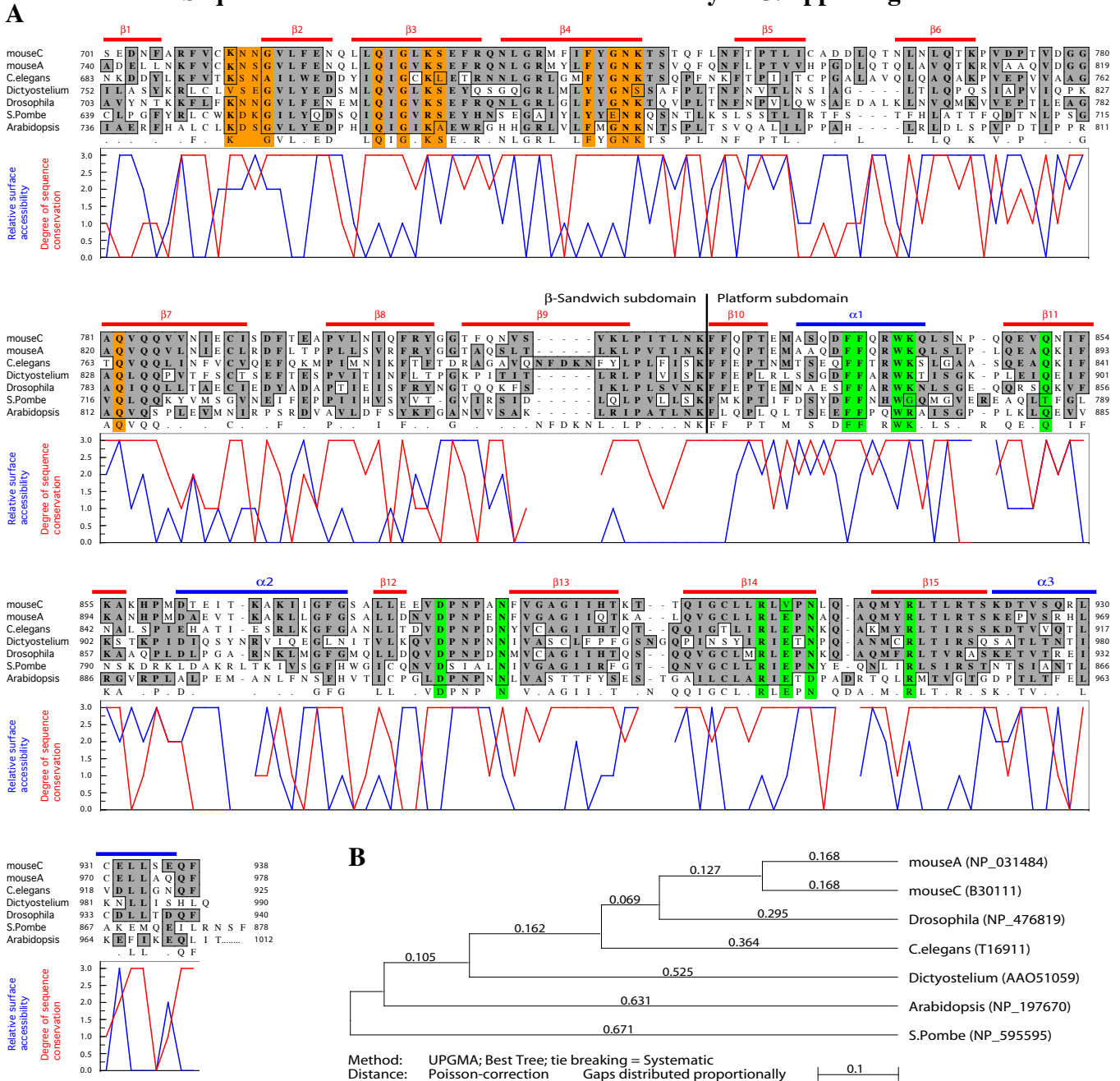
(A) Sequence alignments for various α-adaptin appendages from Mouse to Arabidopsis. β-sheets (red bars) and α-helices (blue bars) from the structure of mouse αC-appendage are plotted and residues involved in binding the WxxF and FxDxF synaptojanin peptides are shaded. Below the alignments we show the degree of conservation (red chart) and the relative surface accessibility (blue chart). Accessibility was calculated for main chain (except Cα), hydrophobic and hydrophilic side chain atoms. The maximum was selected and each data point was binned and normalised onto a 4-point scale 0 - 20, 20.1 - 40, 40.1 - 60, 60+. For sequence conservation the bin categories were 0 - 25, 25.1 - 50, 50.1 - 75, 75.1 - 100. These charts allow conserved surface and structural residues to be distinguished, a feature not readily apparent from simple alignments. Accessible surface area was calculated using the program naccess (Hubbard et al, 1991) (http://wolf.bms.umist.ac.uk/naccess/). Mapping of phylogenetic information onto the structure was carried out using the ConSurf (Glazer et al, 2003) webserver at: http://consurf.tau.ac.il . (B) Phylogenetic tree based on α-adaptin appendage domain sequences from the different genomes. The accession numbers for the proteins shown in A are in brackets.

Hubbard, S. J., Campbell, S. F., Thornton, J. M. (1991) Molecular recognition. Conformational analysis of limited proteolytic sites and serine proteinase protein inhibitors. J. Mol. Biol. *220*, 507-30.

Glaser, F., Pupko, T., Paz, I., Bell, R. E., Bechor-Shental, D., Martz, E. and Ben-Tal, N. (2003) ConSurf: identification of functional regions in proteins by surface-mapping of phylogenetic information. Bioinformatics *19*, 163-164.

Supp Fig. 2
Details of synaptojanin peptide interactions with the α–appendage

Syj-P3 peptide (sequence: *NPKGWVTFEEEE*)

Good density was seen from the Cα of K3 to E9. There are 2 shallow pockets on the β-sandwich subdomain. W5 from the peptide binds into the first pocket with a hydrogen bond being made from the nitrogen on the indole to the main chain carbonyl of G780, which may give specificity to the tryptophan interaction. G742, and methylene units on the side chains of N743, K744 and Q782 provide the core of the pocket. The second pocket is more hydrophobic and contains F8 from the peptide. Space for F8 is created by G725 lying immediately beneath it and the aromatic ring of the peptide interacts with that of F740 by T-shaped π stacking. If these glycines were a larger residue then space in the pocket would be severely restricted. Several asparagines and a lysine are in the vicinity of the acidic C-terminus of the peptide and may contribute to the strength of the interaction by opportunistic hydrogen bonding with the main and side-chains though the weaker density beyond E9 of the peptide make interpretation difficult. The main specificity determinants on the peptide are W, V and F where W is hydrogen bonded, F must be large and hydrophobic and the V position would preferably be a small-uncharged residue because of its close proximity to F740.

Syj-P1 peptide (sequence *LDGFKDSFDLQG*)

Good density was observed from D2 of the peptide to L10. The peptide is oriented by hydrogen bonding from the side chains of R905, E907 and R916 (and K841) and by a series of hydrophobic residues. The peptide F4 is in a strongly hydrophobic environment and W840 forms part of a network of hydrophobic interactions that includes the peptide F4 along with F837 and F836 from the appendage. All four are π-stacked at right angles to one another, thus the importance of the peptide phenylalanine in completion of the network and giving specificity and strength to the interaction. D6 is coordinated by R916 and is hydrogen-bonded to Q851 via a water molecule. S7 of the peptide is hydrogen-bonded to R905. K5 is exposed to the solvent and it would be predicted that several residues may be tolerated at this position; indeed this is E in amphiphysin. There are clear interactions with residues preceding the first phenylalanine which we tested using shorter and longer peptides.
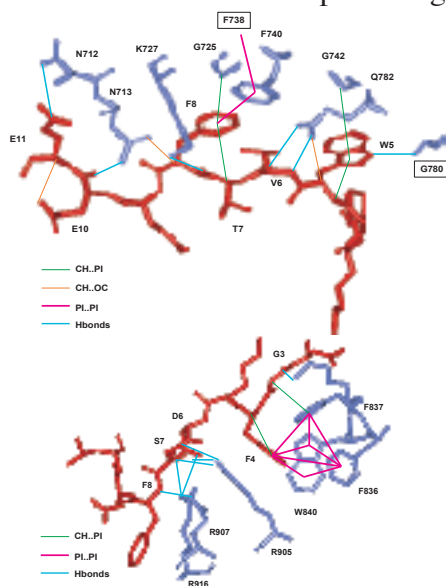
WxxF Synaptojanin P3 peptide

H-bonds:
N712(ND2) to peptide E11(OE2) 3.14Å
N713(ND2) to peptide E10(O) 2.03Å
K727(NZ) to peptide T7 (O) 3.02Å
G780(O) to peptide W5 (NE1) 2.93Å
Q782(OE1) to peptide V6 (N) 2.87Å
Q782(NE2) to peptide V6 (O) 3.2Å

Non canonical:
M:S   CH..PI Peptide T7   to   Peptide F8
M:S   CH..PI Peptide W5   to   Peptide W5
M:S   CH..OC Peptide W5 to   Alpha   Q782
M:S   CH..PI Alpha G742   to   Peptide W5
M:S   CH..OC Peptide E11 to   Peptide E10
M:S   CH..OC Peptide F8   to   Alpha   N713
M:S   CH..PI Alpha G725   to   Peptide F8
M:S   CH..PI Alpha G725   to   Peptide F8
S:S   PI..PI Peptide F8   to   Alpha   F740
M=main chain
S=side chain

FxDxF Synaptojanin P1 peptide

H-bonds:
K841(NZ) to peptide G3(O)   2.75Å SM
R905(NH1) to peptide D6(O)   3.02Å SM
R905(NH2) to peptide D6(O)   3.26Å SM
R905(NH2) to peptide S7(OG) 3.17Å SS
E907(OE2) to peptide F8(N)   2.86Å SM
R916(NH1) to peptide D6(OD2) 3.03Å SS
R916(NH2) to peptide D6(OD1) 2.96Å SS

Non canonical:
M:S   CH..PI peptide F4 to peptide F4
M:S   CH..PI peptide G3 to alpha F837
S:S   PI..PI peptide F4 to alpha F836
S:S   PI..PI peptide F4 to alpha F837
S:S   PI..PI peptide F4 to alpha W840

Non canonical interactions were identified using the program NCI (Madan Babu, 2003) available on our webserver at: http://www.mrc-lmb.cam.ac.uk/genomes/nci/. Hydrogen bonds were identified using HBPLUS (McDonald and Thornton, 1994) available at: http://www.biochem.ucl.ac.uk/bsm/hbplus/ . The WxxF peptide binds like Velcro, where all the interactions along its surface contribute to the affinity of 0.7mM. The FxDxF peptide has 2 distinct interaction sites, one that consists of non-canonical interactions and the other of hydrogen-bonding.

CH..Pi interactions contribute 1 to 1.5kCal/mol; CH..OH interactions contribute 2.5 to 3kCal/mol

Pi..Pi interactions contribute 3.5 to 4kCal/mol; H-bonds contribute on average 5 to 5.5kCal/mol

Madan Babu, M. (2003) NCI - a server to calculate non-canonical interactions in protein structures. Nucleic Acids Research, *31*, 3345-3348.

McDonald, I.K. and Thornton, J.M. (1994), Satisfying Hydrogen Bonding Potential in Proteins. J.M.B. *238*, 777-793.

Supp Fig. 3
Superposition of αC-adaptin and γ-adaptin appendages showing ligand binding residues in γ

A

B

Q769

T770

E797

V800

C

T757

R793

E812

L762

K797
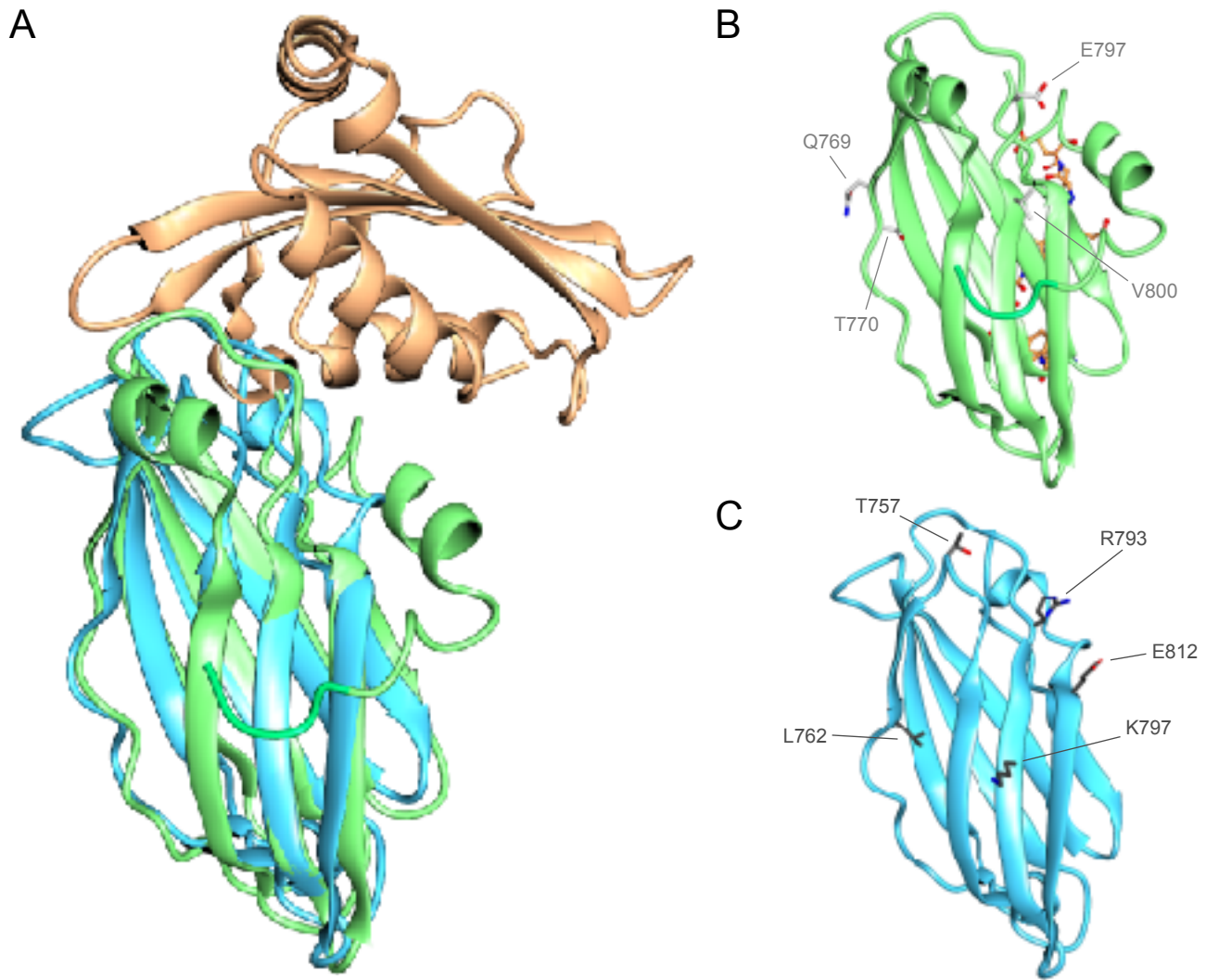
The β-sandwich subdomains of γ and α appendages are superimposed with an rms deviation on Cαs of 1.7Å. The α-appendage is shown in gold and green and the γ-appendage in blue with the g-interaction surface to the fore (DFxDF peptides are displaced by the L762A mutant, Mills et al 2003. In B the WxxF peptide is bound to the opposite face of the β-sandwich subdomain of αC and residues mutated to probe a possible interaction surface like that in the γ-appendage are indicated (C).

Supp Fig. 4
Comparison of WVxF and FxDPW peptides bound to the β-sandwich subdomain
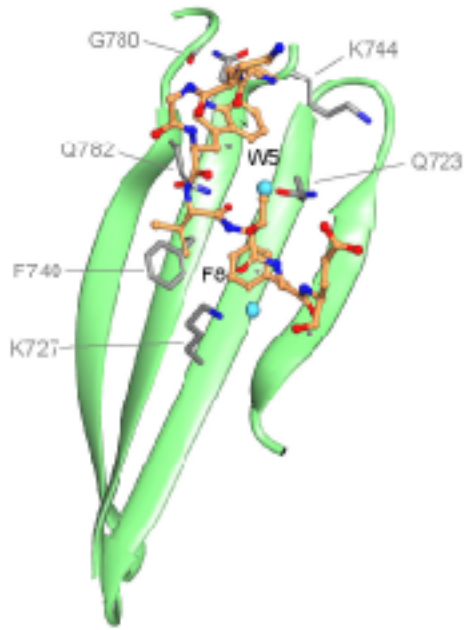
NH2 - N P K G **W V** T **F** E E E E - COOH
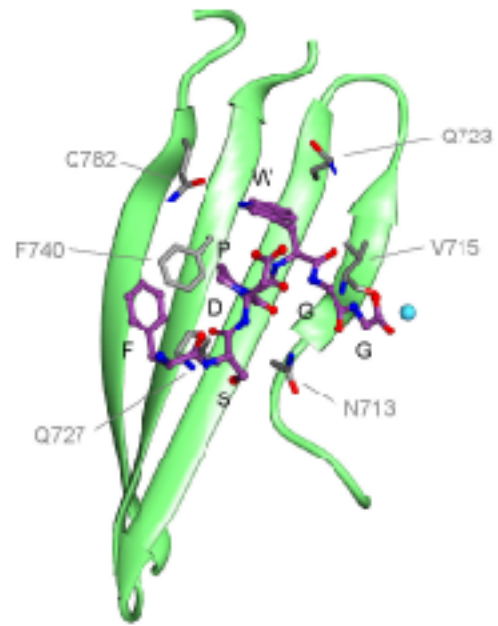
NH2 - F S **D P W** G G - COOH

A DPW peptide from epsin1 (FxDPW) was previously found to bind to the F740 pocket on the β-sandwich subdomain (Brett et al., 2002). This peptide is found at right angles to the WxxF peptide and in our epsin motif-domain experiments and direct peptide affinity measurements it appears that this motif binds very weakly to a-appendage.

Brett, T. J., Traub, L. M., and Fremont, D. H. (2002). Accessory protein recruitment motifs in clathrin-mediated endocytosis. Structure (Camb) 10, 797-809.

Supp Fig. 5
Temperature-dependent enrichment
of accessory proteins in assembly-zones
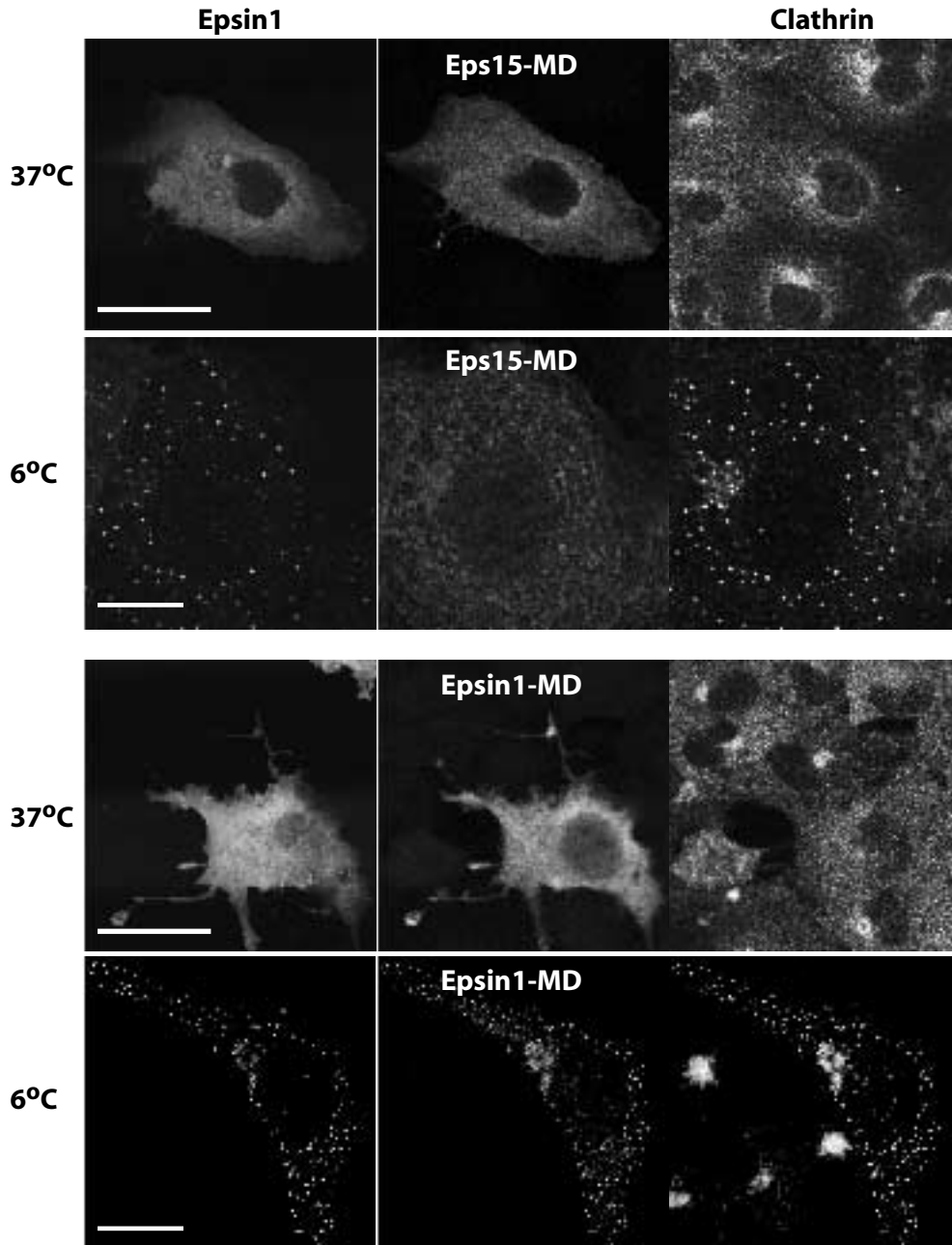
At 37°C there are many clathrin puncta and AP2 adaptor puncta on the cell surface which do not necessarily overlap and the overexpression of the adaptor binding domains (motif domains-MDs) of endocytic protein do not co-localise. In our last publication on epsin1 (Ford et al, 2001) we noted that overexpression of epsin1 full-length protein had either a cytoplasmic distribution or some cells developed large puncta. In the above figure we now show that this punctate distribution is due to a decrease in temperature below 18°C. In the previous paper we did not realise it was due to the fixative being ice-cold and thus some of the cells developed puncta during fixation. These puncta initially are very small but with time they become larger. At all times they are reversible if the cells are warmed again. In the supplementary material of the previous paper we showed that these puncta co-localised with endogenous endocytic components such as eps15 and dynamin. The co-localisation with the motif domains of eps15 and epsin1 is not as striking but this is not surprising given the competition with full-length protein that often have multiple ways to localise to what we call: **assembly-zones**. These zones have been trapped by the low temperature in combination with epsin1 overexpression. This effect is not limited to overexpression of epsin1 (data not shown). Scale bar 20μm.

Ford, M. G., Mills, I. G., Peter, B. J., Vallis, Y., Praefcke, G. J., Evans, P. R., and McMahon, H. T. (2002). Curvature of clathrin-coated pits driven by epsin. Nature *419*, 361-366.

Supp Fig. 6
Epsin1 puncta on the cell surface
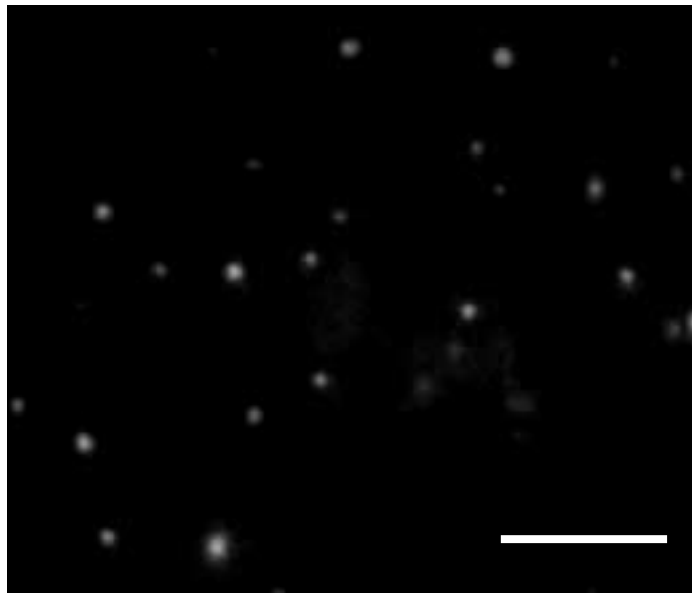
Total internal reflection fluorescence (TIRF) microscopy image of epsin1 expression in COS 7 cells incubated at 6°C. With the settings used we know that the fluorescent spots are on the plasma membrane or within 50nm of the plasma membrane (the illumination field). Using a xz-series we also draw the same conclusion. We can also observe lateral diffusion of the spots and thus these spots are almost certainly plasma membrane associated. Scale bar 10μm.

(We thank Minnie Wu for assistance in capturing this image)

Supp Table1.
Binding partners of the α-appendage determined by liquid chromatography tandem mass spectrometry (LC-MS/MS).

Using LC-MS/MS we can accurately determine the composition of bands that contain mixtures of proteins. We applied this to α-appendage ligands, having washed the samples over a period of 10min. This means that the identification may not be exhaustive as low affinity ligands may easily be displaced. We have used a vast excess of α-appendage over ligands to allow interactions to occur without significant competition. The Coomassie gel used for the analysis tabulated below is shown in the main paper as figure 1C.

Protein	No. of peptides	% coverage of protein		Protein	No. of peptides	% coverage of protein
MAP1A	85	31		MAP2B	25	15
Synaptojanin	18	9		RIP	5	4
Intersectin	24	21		AP180	39	27
Eps15	11	13		AAK	14	26
Amphiphysin1	57	49		Amphiphysin2	16	32
β-adaptin	9	10		Dynamin1	78	58
Dynamin2	11(specific)	26(overall)		Dynamin3	3(specific)	20(overall)
Epsin1	9	13		Epsin2	22	26
Snx9	5	12		Numb-like	6	9
NSF	8	13		HSC70	10	17
HIV-1 Rev BP	14	12		NECAP	6	21

MAP1A, MAP2B, tubulin and 3-phosphoglycerate dehydrogenase were also sequenced from control gels. We know that the MAP1A and MAP2B interactions are not via the same surface as other ligands of the α-appendage as a control mutant in the non-conserved region of the α-appendage (V800D) which we make at a later stage in the paper prevents MAP interactions This mutant does not affect tubulin binding. All the remaining ligands are affected by mutants of conserved ligand-binding surfaces.

We consistently find no clathrin bound directly or indirectly to the α-appendage in these experiments, even after blotting with a clathrin antibody. This would imply that there is no binding site on clathrin for the α-appendage and indirect interactions are too weak.

In figure 1C eps15, amphiphysin and AP180 are found at multiple positions in the gel and these reflect multiple splice forms of the proteins that can bind to the α-appendage.

Sorting nexin 9 (Snx9): Snx9 has an N-terminal SH3 domain that binds to dynamin, SOS, and a number of other proteins containing PxxP sequences (Lundmark and Carlsson, 2003; Schulze and Mann, 2004), a low complexity region that interacts with adaptor complexes and clathrin (Hirst et al., 2003; Lundmark and Carlsson, 2003; Miele et al., 2004), a PX domain that will target the protein to PtdIns(3)P and a C-terminal BAR domain that likely targets the protein to membrane subdomain of high curvature (Peter et al., 2004). The α-appendage interaction in our experiments has been seen before (Lundmark and Carlsson, 2003) where the interaction was suggested to be bivalent. This is indeed likely the case as the PWxxW peptide in figure 4 does not give a sufficiently tight interaction with the α-appendage to be the full story.

Numb-like: Both numb and numb-like proteins bind to beta-amyloid precursor protein (APP) and Notch receptor cytosolic domain (Roncarati et al., 2002). These interactions are mediated by the PTB domains which are also membranes interaction domains. Given the additional interactions of numb with the α-appendage (Santolini et al., 2000) and to clathrin these proteins may thus be important regulators of Notch receptor and APP localization/internalization and thus may be critical for the processing by intramembraneous proteases. The in vivo importance of the α-adaptin:numb interaction have been well demonstrated in Notch signally during asymmetric cell division in Drosophila (Berdnik et al., 2002). The interaction was shown to be via the α-appendage domain and truncations in the platform subdomain and a deletion of 2 conserved buried residues between the 2 subdomains (V824+N825: see Supp Fig. 1A) abolished the interaction. This is consistent with our results that Numb binds to the α-W840 binding pocket on the platform subdomain (Fig. 1D) and the presence of an FxxFxxL motif that interacts with the appendage (data not shown, but see Fig. 4 for the interaction site for this motif).

Epsin2: Both epsin1 and epsin2 are brain enriched, found in coated vesicles, and bind to AP2 adaptors (Rosenthal et al., 1999). The N-terminal domain (ENTH domain) binds to PtdIns(4,5)P_2 and this interaction induces the folding of an additional helix that inserts into the membrane resulting in an increase in membrane curvature (Ford et al., 2002). Epsin also promotes clathrin polymerisation and thus the membrane bending capability is stabilised by the clathrin lattice formation. Epsins are also critical in the recruitment of AP2 adaptors to the membrane (Ford et al., 2002) and have several ubiquitin interaction motifs, and thus it appears that epsins may be key regulator of CCV formation. The differences between epsins 1 and 2 are mostly in the sequence of the motif domain but clathrin, eps15 and AP2 adaptor motifs are all preserved. Thus it is likely that these 2 proteins may be functionally redundant if expressed in the same neuron.

Dynamins: It was initially surprising to us to find such an intense band of dynamin in an α-appendage pull-down. With more intense washing of the α-appendage beads then most of the dynamin dissociates while still leaving the other major interaction partners. We have previously shown that this interaction is at least in part binding to the SH3 domains of amphiphysins 1 and 2 (Owen et al., 1999), however we also note in our current experiments with mutants of the α-appendage that the interaction of amphiphysin does not precisely parallel the dynamin interaction and this would agree with an additional direct interaction between dynamin and the α-appendage as previously published (Wang et al., 1995). It is interesting that a DxF motif in the proline rich domain of dynamins 1, 2 and 3 is conserved. Thus dynamin interactions may be localised not only by amphiphysin but in addition by AP2 adaptors.

AAK: Casein kinase2 (CK2), GAK/auxilin2 and adaptor-associated kinase (AAK) are all CCV-associated kinases (Conner and Schmid, 2002; Korolchuk and Banting, 2002). In figure 1 we find that AAK is enriched by the α-appendage but even more so by the clathrin terminal domain.

NSF: It is not clear to us why we have identified this protein but there is a single DxF motif in the N-terminus and in the same pull-down we also find a protein similar to γ-SNAP associated factor 1, also call Rab11-interacting protein (see below).

Rab11-interacting protein: This protein is implicated in the sorting and trafficking of protein in the endosomal system. It has a WxDNF sequence and was detected as part of 2 separate bands but the number of peptides were low and thus it is

not highly enriched and thus we cannot be certain of the importance of this α-interaction partner.

NECAP: NECAP (adaptin-ear-binding coat-associated protein) 1 and 2 have previously been shown to bind to the α-appendage via a WVQF motif (Ritter et al., 2003). In this paper we identify the binding site for this motif on the β-sandwich subdomain of the α-appendage. The function of this protein family is not known.

HIV-1 Rev binding/interacting protein (RIP): The Rev protein facilitates the nuclear export of viral RNA, by binding to the RNA via an RNA binding domain and to components of the export pathway via an effector domain (Fritz et al., 1995). The Rev binding protein has an ArfGAP domain and multiple FG repeats important for nucleocytoplasmic transport. It has 2 DxF motifs and multiple FxxFxxØ motifs that may interact directly with AP2 adaptors. It also has multiple NPF motifs and has previously been isolated in a screen using the Eps15-homology (EH) domains of intersectin (Yamabhai et al., 1998), a protein that also interacts directly with the α-appendage. Our peptides only cover the predicted 60kDa form of this protein. The ability of HIV viruses to control clathrin-mediated endocytosis is implied and needs to be studied.

Berdnik, D., Torok, T., Gonzalez-Gaitan, M., and Knoblich, J. A. (2002). The endocytic protein alpha-Adaptin is required for numb-mediated asymmetric cell division in Drosophila. Dev Cell *3*, 221-231.

Conner, S. D., and Schmid, S. L. (2002). Identification of an adaptor-associated kinase, AAK1, as a regulator of clathrin-mediated endocytosis. J Cell Biol *156*, 921-929.

Ford, M. G., Mills, I. G., Peter, B. J., Vallis, Y., Praefcke, G. J., Evans, P. R., and McMahon, H. T. (2002). Curvature of clathrin-coated pits driven by epsin. Nature *419*, 361-366.

Fritz, C. C., Zapp, M. L., and Green, M. R. (1995). A human nucleoporin-like protein that specifically interacts with HIV Rev. Nature *376*, 530-533.

Hirst, J., Motley, A., Harasaki, K., Peak Chew, S. Y., and Robinson, M. S. (2003). EpsinR: an ENTH domain-containing protein that interacts with AP-1. Mol Biol Cell *14*, 625-641.

Korolchuk, V. I., and Banting, G. (2002). CK2 and GAK/auxilin2 are major protein kinases in clathrin-coated vesicles. Traffic *3*, 428-439.

Lundmark, R., and Carlsson, S. R. (2003). Sorting nexin 9 participates in clathrin-mediated endocytosis through interactions with the core components. J Biol Chem *278*, 46772-46781.

Miele, A. E., Watson, P. J., Evans, P. R., Traub, L. M., and Owen, D. J. (2004). Two distinct interaction motifs in amphiphysin bind two independent sites on the clathrin terminal domain beta-propeller. Nat Struct Mol Biol *11*, 242-248.

Owen, D. J., Vallis, Y., Noble, M. E., Hunter, J. B., Dafforn, T. R., Evans, P. R., and McMahon, H. T. (1999). A structural explanation for the binding of multiple ligands by the alpha-adaptin appendage domain. Cell *97*, 805-815.

Peter, B. J., Kent, H. M., Mills, I. G., Vallis, Y., Butler, P. J., Evans, P. R., and McMahon, H. T. (2004). BAR domains as sensors of membrane curvature: the amphiphysin BAR structure. Science *303*, 495-499.

Ritter, B., Philie, J., Girard, M., Tung, E. C., Blondeau, F., and McPherson, P. S. (2003). Identification of a family of endocytic proteins that define a new alpha-adaptin ear-binding motif. EMBO Rep *4*, 1089-1095.

Roncarati, R., Sestan, N., Scheinfeld, M. H., Berechid, B. E., Lopez, P. A., Meucci, O., McGlade, J. C., Rakic, P., and D'Adamio, L. (2002). The gamma-secretase-generated intracellular domain of beta-amyloid precursor protein binds Numb and inhibits Notch signaling. Proc Natl Acad Sci U S A *99*, 7102-7107.

Rosenthal, J. A., Chen, H., Slepnev, V. I., Pellegrini, L., Salcini, A. E., Di Fiore, P. P., and De Camilli, P. (1999). The epsins define a family of proteins that interact with components of the clathrin coat and contain a new protein module. J Biol Chem *274*, 33959-33965.

Santolini, E., Puri, C., Salcini, A. E., Gagliani, M. C., Pelicci, P. G., Tacchetti, C., and Di Fiore, P. P. (2000). Numb is an endocytic protein. J Cell Biol *151*, 1345-1352.

Schulze, W. X., and Mann, M. (2004). A novel proteomic screen for peptide-protein interactions. J Biol Chem *279*, 10756-10764.

Wang, L. H., Sudhof, T. C., and Anderson, R. G. (1995). The appendage domain of alpha-adaptin is a high affinity binding site for dynamin. J Biol Chem *270*, 10079-10083.

Yamabhai, M., Hoffman, N. G., Hardison, N. L., McPherson, P. S., Castagnoli, L., Cesareni, G., and Kay, B. K. (1998). Intersectin, a novel adaptor protein with two Eps15 homology and five Src homology 3 domains. J Biol Chem *273*, 31401-31407.

Supp Table 2
Crystallographic statistics

Spacegroup	C2
Resolution (Å)	39.53 – 1.90 (2.00 – 1.90)
Completeness (%)	0.951 (0.737)
Multiplicity	3.4 (2.1)
Average Intensity (I)	5472 (366)
Sigma (σ)	805.2 (506.1)
Mean I / σ	12.1 (1.8)
Wilson Plot B (Å^2)	27.282
Rmerge (%)	0.077 (0.651)
Rmeas (%)*	0.089 (0.868)

  *Rmeas is the multiplicity-weighted Rmerge   Brackets – high resolution bin
Refinement statistics

R factor (%)	0.177
R_{Free} (%)	0.224
R_{Free} test set size (%)	0.051
<B> Å^2 (mean, overall)	27.98
$N_{reflections}$ (N_{free})	27464 (1467)
N_{atoms} (N_{water})	2467 (297)
R_{msd} bond length (Å)	0.03
R_{msd} bond angles (°)	2.2

Data collection statistics for the intensities collected at ID 14.1 ($\lambda = 0.98\text{Å}$) at the European Synchrotron radiation Facility in Grenoble, France. Crystals were monoclinic and belonged to spacegroup C2 (a = 146.6Å, b = 67.3Å, c = 39.7Å, β = 94.53°). Synchrotron data were recorded using an ADSC charge-coupled device detector.

Reflections were integrated using MOSFLM (Leslie, 1992) and were scaled using SCALA from the CCP4 crystallographic suite (Collaborative Computational Project, 1994). Phases were determined using AmoRe (Navaza, 2001), using the previously published structure of the ligand-free α-adaptin appendage (Owen et al., 1999) (PDB id: 1B9K) as a search model. The structure was completed using O (Jones et al., 1991) and refined using Refmac5 (Murshudov et al., 1997). The validated structure has been deposited with the Protein Data Bank (Berman et al., 2000) with the id XXX.

All structural diagrams were generated with Aesop (Martin Noble, unpublished) and the schematics of peptide interactions were generated using the LigPlot output as a starting point (Wallace et al., 1995).

Berman, H. M., Westbrook, J., Feng, Z., Gilliland, G., Bhat, T. N., Weissig, H., Shindyalov, I. N., and Bourne, P. E. (2000). The Protein Data Bank. Nucleic Acids Res. *28*, 235-242.

Collaborative Computational Project, N. (1994). The CCP4 suite: programs for protein crystallography. Acta Cryst. *D50*, 760-763.

Jones, T. A., Zou, J. Y., Cowan, S. W., and Kjeldgaard, M. (1991). Improved methods for building protein models in electron density maps and the location of errors in these models. Acta Cryst. *A47*, 110-119.

Leslie, A. G. W. (1992). Recent changes to the MOSFLM package for processing film and image plate data. In Joint CCP4 and ESF-EACMB Newsletter on Protein Crystallography No. 26 (SERC, Daresbury Laboratory, Warrington, UK).

Murshudov, G. N., Vagin, A. A., and Dodson, E. J. (1997). Refinement of Macromolecular Structures by the Maximum-Likelihood Method. Acta Cryst. *D53*, 240-255.

Navaza, J. (2001). Implementation of molecular replacement in AMoRe. Acta Cryst. *D57*, 1367-1372.

Owen, D. J., Vallis, Y., Noble, M. E., Hunter, J. B., Dafforn, T. R., Evans, P. R., and McMahon, H. T. (1999). A structural explanation for the binding of multiple ligands by the alpha-adaptin appendage domain. Cell *97*, 805-815.

Wallace, A. C., Laskowski, R. A., and Thornton, J. M. (1995). LIGPLOT: a program to generate schematic diagrams of protein-ligand interactions. Protein Eng. *8*, 127-134.

Supp Table 3
ITC parameters for peptide affinity measurements

Peptide	Sequence	Peptide binding to α-adaptin wild-type appendage				
		$K_d(\mu M)$	[Peptide/ appendage]	$K_a(M^{-1})$	ΔH(kcal mol^{-1})	$T\Delta S$(kcal mol^{-1})
Syj-P1	LDGFKDSFDLQG	28.6 ± 3.8	0.9 (2 obs.)	3.65e4 ± 5.7e3	-14.3 ± 0.6	-8.4 ± 0.8
Syj-P2	LDGFEDNFDLQG	4.5 (2 obs.)	1.3±0.2	2.23e4 ± 1.7e2	-11.9 ± 0.3	-5.0 ± 0.4
Amph-P1	FEDNFVP	20.9 ± 2.2	1.2 ± 0.1	4.83e4 ± 5.1e3	-6.9 ± 0.2	-0.9 ± 0.1
Amph-P1mut	FERNFVP	No binding				
Amph-P2	INFFEDNFVPEI	2.5 ± 0.3	1.1 ± 0.1	3.98e5 ± 4.7e3	-9.9 ± 0.9	-2.5 ± 0.8
Amph-P3	ASLLDLDFEPLPP VASPVKAPTTSG QSIPWDLWE	179.0 ± 38	2.0 (2 obs.)	5.85e3 ± 1.2e3	-11.7 ± 0.3	-6.9 ± 0.5
Epsin1-P	APAFSDPWGGSP	200.0	1.2	5.0e3	-10.0	-5.2
Syj-P3	NPKGWVTFEEEE	0.72 ± 0.1	0.8 ± 0.1	1.43e6 ± 3.0e5	-15.6 ± 0.4	-7.6 ± 0.3
NECAP-P1	QAPQPSNWVQF	7.5 ± 0.5	0.9 (2 obs.)	1.34e5 ± 7.6e3	-15.2 ± 0.3	-8.6 ± 0.3
Snx9-P1	GNDPWSAWSASK	161	1.1	6.20e3	-11.0	-6.1
EpsinR-P3 (Mills *et al.*)	SADLFGGFADFG	73.5 ± 14.5	1.1 (2 obs.)	1.41e4 ± 2.8e3	-7.7 ± 0.4	-2.3 ± 0.5
Eps15-P1	SFGDGFADFSTL	127.0 ± 24	0.9 ± 0.1	8.03e3 ± 1.4e3	-9.7 ± 3.0	-5.2 ± 3.1
Eps15-P2	SFGGGFADFSTL	119	0.6	8.4e3	-14.0	-8.8
Numb-P1	RQGSFRGFPALS	206.5 ± 64	1.1 ± 0.6	7.00e3 ± 2.4e3	-0.68 ± 0.1	4.3 ± 0.04
Intersectin2-P1	EVWVRFDLQLFE	11.0	2.8 (inaccurate due to limited solubility of peptide)	9.14e4	-20.2	-13.8
		Peptide binding to α-adaptin F740D appendage				
Amph-P2		2.5 ± 0.1	1.2 ± 0.1	3.98e5 ± 12.1e4	-9.7 ± 0.04	-2.4 ± 0.05
Amph-P3		207	0.4	4.83e3	-14.1	-9.4
Syj-P3		167	1.7	5.99e3	-1.3	3.6
Syj-P4		123	0.9	8.1e3	-2.9	2.2
Eps15-P1		85	1.1	1.18e4	-11.1	-5.8
Eps15-P2		107	0.8	9.4e3	-8.9	-3.8
		Peptide binding to α-adaptin G725E+G742D appendage				
Eps15-P2		132	0.7	7.6e3	-12.0	-7.0
Syj-P4		171	1.0	5.8e3	-3.2	1.7
		Peptide binding to α-adaptin G742D appendage				
Eps15-P1		82	0.9	1.22e4	-6.8	-1.5

		Peptide binding to α-adaptin W840A appendage			
Amph-P2		79	0.3 (W840 mutant sometimes precipitates, see also below)	1.26e4	-8.7	-3.3
Syj-P3		0.42 ± 0.2	1.2 ± 0.1	2.72e6 ± 9.5e5	-16.4 ± 0.3	-8.1 (2 obs)
Eps15-P1		43.0	0.5(inaccurate)	2.34e4	-3.7	1.9
Eps15-P2		No binding				
Numb-P1		No binding				
		Peptide binding to α-adaptin V800D appendage			
Amph-P2		1.9	1.1	5.30e5	-9.0	-1.6
Eps15-P2		135.0	0.7	7.43e3	-10.1	-5.1
Syj-P3		0.82	1.1	1.21e6	-15.8	-7.9
		Peptide binding to β2-adaptin			
Syj-P1		No binding				
Amph-P2		No binding				
Epsin1-P1		830.0	2.0	1.21e3	-7.1	-3.1
EpsinR-P3 (Mills *et al.*)		87.0 ± 15	1.2 ± 0.1	1.18e4 ± 2.1e3	-8.3 ± 0.05	-3.0 ± 0.2
Eps15-P1		45.7 ± 5	1.1 ± 0.1	2.21e4 ± 2.6e3	-6.6 ± 0.2	-1.0 ± 0.2
Eps15-P2		57.8	1.1	1.73e4	-9.3	-3.8
Syj-P3		616.0 ± 124	0.8 ± 0.3	1.70e3 ± 3.4e2	-8.2 ± 0.6	-4.0 ± 0.5

Where more than one measurement was made we give the mean ± range

Supp Table 4
ITC parameters for protein affinity measurements

Protein		Protein binding to α-adaptin WT appendage				
Protein		K_d(µM)	[Appendage/ protein]	K_a(M^{-1})	ΔH(kcal mol^{-1})	TΔS(kcal mol^{-1})
Eps15-MD-C1 (C1:530-896)	1st site	0.034	0.5	2.97e7	-20.6	-11.0
	Other sites	21.0	2.1	4.71e4	-18.6	-12.6
Eps15-MD (GST) (C6:530-791)	1st site	0.021 ± 0.001	0.8 ± 0.1	4.86e7 ± 1.3e6	-21.6 ± 1.5	-11.6 ± 1.5
	Other sites	15.7 ± 1.5	2.6 ± 0.1	6.43e4 ± 6.3e3	-18.0 ± 0.8	-11.7 ± 0.8
Eps15-MD (6xHis) (C6:530-791)	1st site	0.020	1.0	5.08e7	-22.6	-12.6
	Other sites	11.0	3.1	9.24e4	-17.1	-10.7
Epsin-MD (6xHis)	1st site	1.0 ± 0.2	0.9 ± 0.1	9.82e5 ± 2.0e5	-19.2 ± 0.4	-11.4 ± 0.5
	Other sites	39.7 ± 1.7	1.8 ± 0.1	2.53e4 ± 1.1e3	-22.4 ± 3.7	-16.7 ± 3.8
Epsin-MD+ (GST)	1st site	0.16	1.2	6.24e6	-20.2	-11.4
	Other sites	5.1	2.5	1.94e5	-14.0	-7.2
AP180-MD (516-915)	1st site	3.6	1.0	2.76e5	-12.4	-5.4
	Other site	46.3 although this does not fit accurately	1.9	2.16e4	-9.1	-3.5
Syj170-MD (1310-1574)	1st site	0.03 ± 0.01	1.2 ± 0.1	3.81e7 ± 1.35e7	-26.1 ± 1.5	-16.3 ± 1.2
	Other site	46.0	1.5	2.18e4	-15.0	-9.4
Syj170-MD mut (1310-1574) DPF → DPD	1st site	0.017	0.7	6.03e7	-28.3	-18.2
	Other site Insecure fit	17.0	0.2	5.7e4	-49.3	-43.3
		Protein binding to α-adaptin F740D appendage				
Eps15-MD (GST) (C6:530-791)		18.9	2.4	5.29e4	-11.4	-5.3
Epsin-MD+ (GST)		15.6	2.8	6.42e6	-20.0	-13.7
AP180-MD (516-915)		96.0	1.8	1.04e4	-23.8	-18.6
		Protein binding to α-adaptin G742D appendage				
Eps15-MD (GST) (C6:530-791)		17.0	0.8	5.86e4	-17.8	-11.6
		Protein binding to α-adaptin W840A appendage				
Eps15- MD (GST) (C6:530-791)	1st site	1.2	0.6	8.59e5	-9.7	-2.0

	Other sites	Intermediate affinity sites are gone leaving mM background affinity. This background is likely present with α-Wt and the α-F740D mutant but gets incorporated into the intermediate affinity site. This shows the difficulty in distinguishing different affinity sites if we do not see the inflection points in the trace and if the affinities are low.				
Epsin-MD+ (GST)		90.0	2.8	1.11e4	-14.5	-9.3
AP180-MD (516-915)		70.0 (hard to fit)	1.6	1.4e4	-5.6	-0.2
Syj170-MD (1310 – 1574)		0.4	0.8	2.7e6	-12.5	-14.5
		Protein binding to β2-adaptin wild-type appendage				
Eps15-MD (6xHis) (C6:530-791)	1st site	0.57	0.9	1.76e6	-17.1	-9.1
	Other site	30.0	1.0	3.33e4	-14.1	-8.2
Epsin-MD (6xHis)	1st site	45.0	1.5	2.21e4	-17.7	-12.1
Epsin-MD+ (GST)	1st site	39.0	1.4	2.64e4	-27.1	-21.3

Where more than one measurement was made we give the mean ± range